Ab initio theoretical study on the reactions of a hydrogen molecule with small platinum clusters: A model for chemisorption on a Pt surface

H. Nakatsuji, Y. Matsuzaki, and T. Yonezawa
Division of Molecular Engineering, Graduate School of Engineering, Kyoto University, Kyoto 606, Japan

(Received 1 June 1987; accepted 27 January 1988)

Reactions of a hydrogen molecule with small platinum clusters Pt_n ($n = 1,2,3$) are studied theoretically by *ab initio* methods. This provides a cluster model study for hydrogen chemisorption on a Pt surface. The results suggest that the Pt atom and the linear Pt_3 cluster will react with H_2 and dissociatively adsorb it, making two Pt–H bonds, whereas the Pt_2 cluster will not react with H_2 because of a high energy barrier. The dissociative adsorption of a hydrogen molecule occurs at a side-on, on-top site of a surface Pt atom and molecular adsorption does not seem to occur. Essentially only one Pt atom is involved in the initial adsorption process. These findings are in contrast to the palladium case previously reported. Almost no energy barrier exists for the hydrogen migration from one Pt atom to an adjacent one, with a preference being shown for one H atom on each Pt atom rather than two H atoms on one Pt atom. The heat of adsorption, the stability of the catalytic surface, etc., are best represented by the Pt_3–H_2 system. Spin–orbit coupling effect is examined for the Pt–H_2 system and found to be small for the singlet A_1 state which is the most important state for the dissociative adsorption. This effect is important, however, to obtain natural potential curve in the large Pt–H_2 separation.

I. INTRODUCTION

Clarification of the electronic processes in the dissociation of a chemical bond of an admolecule on a metal surface is very important in the study of heterogeneous catalysis. Reactivities of small metal clusters are also a recent topic of cluster chemistry.

The interaction of H_2 with a single Ni atom has been studied by Blomberg and Siegbahn.[1] Only the singlet excited state of the Ni atom leads to a bent equilibrium geometry with the H–H distance being almost twice as large as that of a free H_2 molecule. Siegbahn *et al.* have further investigated the dissociation of H_2 on the Ni (100) surface at both on-top and bridge sites using Ni_{14} and Ni_{13} clusters, respectively.[2] The preference of the on-top, side-on site and the importance of the 3*d* electrons in the process have been clarified.

The interaction of an H_2 molecule with the Pd_2 cluster has been investigated in our laboratory as a model of hydrogen chemisorption on a Pd surface.[3,4] The side-on bridge-site approach is preferable and both molecular and dissociative forms seem to exist with the latter being more stable by a few kcal/mol. On the other hand, a single Pd atom is not active enough to cleave the H–H bond.[4,5] Furthermore, we have studied the catalytic activity of palladium for the hydrogenation reaction of acetylene into ethylene.[6] Both Eley–Rideal and Langmuir–Hinshelwood mechanisms were examined. The hydrogen atom dissociatively adsorbed on Pd was shown to be very reactive for acetylene.

Several theoretical studies on the electronic structures and the natures of bondings involved in platinum–atomic hydrogen systems and platinum–molecular hydrogen systems have been reported.[7–9] Wang and Pitzer[7] studied the electronic structures of PtH and PtH^+ by a relativistic *ab initio* method and concluded that the bonding involves both 5*d* and 6*s* electrons. The electronic structures of the Pt clusters Pt_n and their interactions with H in Pt_n–H ($n = 1$–4) system were reported by Gavezzotti *et al.*[8] Their calculations were performed by an *ab initio* pseudopotential SCF MO method without relativistic corrections and correlation effects. The binding energies of a hydrogen atom to Pt clusters and the energy barrier for hydrogen to reach the center of the tetrahedral cavity in the Pt_4H system were investigated. The only *ab initio* theoretical study reported so far for the interaction of a molecular hydrogen with a platinum cluster is the Pt–H_2 system reported by Poulain *et al.*[9] They stated that the electronic state responsible for the capture of H_2 is the closed-shell singlet A_1 excited state. The equilibrium geometry of the system corresponds to a broken H–H bond with an HPtH angle of about 100°. On the other hand, several theoretical studies have been made on the oxidative addition of H_2 to a Pt complex such as $Pt(PH_3)_2$.[10] The electronic mechanism for hydrogen addition in this system is essentially the same as that for a bare platinum atom.[9] Miyoshi *et al.* have studied the electronic structure of the Pt_4 cluster.[11]

Experimentally, Tsuchiya *et al.*[12] have studied the chemisorption of hydrogen on a platinum black catalyst by the TPD (Temperature Programmed Desorption) technique. They reported that at least four different states exist for the hydrogen chemisorbed on platinum, based on the appearance of four TPD peaks. Furthermore, they investigated the reactivity of these various types of chemisorbed hydrogens for the hydrogenation of ethylene.[13] On the other hand, Christmann *et al.* have reported that on the Pt(111) surface the adsorption is completely dissociative at -120 °C.[14] Bernasek and Somorjai[15] and Salmeron *et al.*[16] have studied the H_2–D_2 exchange reaction on the step and terrace sites of a platinum crystal surface.

In this paper, we examine the electronic structures of the Pt_n clusters ($n = 1,2,3$) and their reactions with a hy-

 0021-9606/88/095759-11$02.10

drogen molecule. The main purpose is to provide a model study for clarifying the electronic processes of chemisorptions and catalytic actions on a metal surface, though cluster chemistry itself is also of considerable interest. First, we describe the interaction of an H_2 molecule with a single Pt atom, not only for the ground state, but also for some lower-lying excited states. We examine the effect of spin–orbit coupling for the potential energy curves of these states. Two approaches of H_2 to the Pt atom are considered; viz., side-on and end-on. Since the side-on approach seems to be the most preferable one, we examine only this approach for the larger clusters Pt_2 and Pt_3. For Pt_2, both on-top and bridge sites are studied for the side-on approach. We examine the energetics and the mechanism of H atom migration to an adjacent Pt atom. Finally, the stability of the Pt–Pt bond during the interaction with hydrogen is investigated.

II. COMPUTATIONAL METHOD

The Gaussian basis set for the Pt atom is the $(4s4p5d)/[3s2p2d]$ set and the Xe core is replaced by the relativistic effective core potential.[17] For hydrogen, we use the $(4s)/[2s]$ set of Huzinaga–Dunning,[18] plus p-type functions which are the first derivatives of the $[2s]$ set. Then, the Hellmann–Feynman theorem is essentially satisfied for the forces acting on the hydrogen nuclei.[19] In the present study, we examine paths of approach, cleavage of the hydrogen molecule, and migration of H atoms on the Pt_n cluster with the Pt–Pt distance fixed. So, we are primarily interested in the forces acting on the protons of H_2. The calculated Hellmann–Feynman forces are thus conveniently used in the optimization processes. This is also in agreement with the finding of Wang and Pitzer[7] for PtH that the polarization functions centered on the H atom are more important than those centered on the Pt atom. For the Pt–H_2 system, the optimized path is calculated by the Hartree–Fock (HF) method. The potential energy curves of the ground and excited states are calculated by the SAC (symmetry adapted cluster)[20] and SAC-CI[21] methods. The linked operators in the SAC and SAC-CI calculations are selected using the thresholds λ_g and λ_e of 1×10^{-5} and 5×10^{-5} a.u., respectively.[22] The wave function consists of 500–1200 linked operators which are symmetry adapted in each spin symmetry. Details of the algorithm for the SAC and SAC-CI calculations have been reported elsewhere.[21–23] Other potential energy curves of the Pt–H_2 system and all of the potential energies of the Pt_2, Pt_3, and Pt_2–H_2 systems are calculated by the CASSCF method[24] and those of the Pt_3–H_2 system are calculated by the MC-SCF method. For the Pt_3–H_2 system, the MC-SCF orbitals are optimized within the lower 61 orbital space with the upper 18 orbitals being frozen to those of the HF method.[25] The SCF calculations were performed with the use of the program GAMESS,[26] modified for the present purpose.[25]

The effect of the spin–orbit coupling is examined for the Pt–H_2 system. It is included for the ground and excited states obtained by the SAC/SAC-CI method through

$$H_{IJ} = E_I\delta_{IJ} + V_{IJ}^{SO}, \tag{1}$$

where E_I is the energy of the SAC/SAC-CI method and V_{IJ}^{SO} is the matrix element of the spin–orbit coupling operator defined by[27]

$$V_{IJ}^{SO} = \langle I|H^{SO}|J\rangle, \tag{2}$$

$$H^{SO} = \frac{\alpha^2}{2}\sum_i\sum_A \frac{Z_A}{r_{iA}^3} l_i s_i. \tag{3}$$

We calculate the integral V_{IJ}^{SO}, considering only the spin–orbit coupling in Pt, and the state functions I and J are approximated by the Hartree–Fock and single excitation CI functions. The spin–orbit coupling constant for the d orbitals of the Pt atom is estimated as 0.0153 a.u. (9.6 kcal/mol) from the atomic spectral data.[28]

III. Pt–H_2 SYSTEM

A. Side-on, on-top approach

We first examine the side-on, on-top approach of a hydrogen molecule to a Pt atom. In this section, we do not include the effect of the spin–orbit coupling. This effect will be examined in Sec. III B. The definition of the reaction path is shown in Table I and Fig. 1. In this system, only the central Pt atom (denoted as Pt_a) is considered. At the initial points 1 and 2, the H–H distance is fixed at the equilibrium length, 0.741 Å, of a free hydrogen molecule.[29] At the points 3, 4, and 5, it is optimized by the HF method. At the points 6 and 7, the Pt–H distance is fixed at 1.53 Å, which is the observed bond length of the free Pt–H molecule,[29] and the H_2 is located on the circle as shown in Fig. 1. The most stable geometry of the Pt–H_2 system, calculated by the HF method, is indicated by the open circles. The calculated H–H distance 2.05 Å is almost three times as long as that of a free hydrogen molecule, while the Pt–H distance 1.46 Å is slightly shorter than the bond distance 1.53 Å of the free Pt–H molecule. The corresponding H–H distances for the Pd–H_2 and Ni–H_2 systems have been reported to be 0.768 Å[4] and 1.271 Å,[1] respectively, the former corresponding to molecular adsorption and the latter to dissociative adsorption, although in the Ni–H_2 system some H–H bonding still remains.[1]

Figure 2 is a display of the forces acting on the H atoms of the Pt–H_2 system along the reaction path calculated from the HF wave function. At all the points, 1–6, the H atoms are attracted by the Pt atom. At the point 2, the H_2 molecule experiences the forces which act to elongate the H–H distance. At the points 3–5, that force is zero because the H–H distance has been optimized. At the point 7, the H atoms are repelled by the Pt atom. The optimized position of H_2 (open circles, Fig. 1) is a little bit inside of the position 6, as indicated from the force.

TABLE I. Reaction path for the Pt–H_2 system.

Position	$R_{Pt\text{-}H_2}(A)$	$R_{H\text{-}H}(A)$	
1	2.600	0.741	Fixed at $R_{eq}(H_2)$
2	2.150	0.741	
3	1.700	0.842	Optimized
4	1.530	1.000	
5	1.300	1.600	
6	1.082	2.164	$R_{PtH} = R_{eq}(PtH) = 1.53$ Å
7	0.586	2.827	

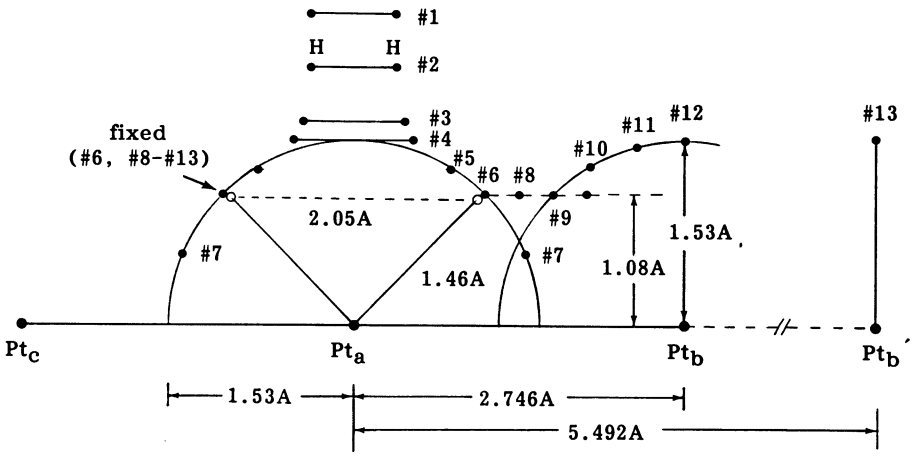

FIG. 1. Reaction path for the Pt_n–H_2 ($n = 1,2,3$) system and the most stable geometry for the Pt–H_2 system shown by the open circles.

The potential energy curves of the Pt–H_2 system calculated by the SAC and SAC-CI methods are shown in Fig. 3. The $^1A_1$ state is calculated by the SAC method and the other triplet excited states, by the SAC-CI method. They are calculated along the path shown in Fig. 1. The ground state of the Pt atom is $^3D(d^9s^1)$. The closed shell $^1S(d^{10})$ state is calculated to be about 23.5 kcal/mol above this state; by comparison the experimental value for this is 17.5 kcal/mol.[28] All the triplet states arising from the ground state (^3D) of the Pt atom show large energy barriers of more than 16 kcal/mol (B_1, A_2, and B_2 states) with the stabilization energies less than 10 kcal/mol (B_2 state). Only the $^1A_1$ state, which originates from the excited ^1S state of the Pt atom, is very attractive. The calculated stabilization energy of the $^1A_1$ state, relative to the dissociation limit of Pt(^3D) + H_2, is about 40 kcal/mol, which is larger than the experimental heat of adsorption, 26 kcal/mol.[30] In the dissociative adsorption process, the spin–orbit interaction is important, as shown below, particularly near the crossing point between the singlet and triplet curves. When Pt–H_2 takes a linear form, the $^3\Delta_g$ state is most stable, but it is about 37 kcal/mol higher than the bent $^1A_1$ equilibrium geometry. Poulain *et al.* also obtained a similar result.[9] Based on the atomic spectra,[28] the $^3F(d^8s^2)$ state of the Pt atom is only 2.4 kcal/mol above the ^3D ground state. The potential energy curves for the interaction of this state with H_2 are calculated by the CASSCF method and plotted in Fig. 4. When the Pt–H_2 distance is large, all the states arising from the ^3F state of Pt are not attractive, so that this state seems to be unimportant for the H_2 capture by Pt. We thus conclude that even a single Pt atom leads to a dissociative adsorption of the H_2 molecule. The catalytically active state for this adsorption is not the ground state, but the excited ^1S state of the Pt atom. When we consider the spin–orbit interaction, as in Sec. III B, we get the more natural potential curves in the region of large Pt–H_2 distance. On the basis of the present calculations, a molecular adsorption state does not seem to exist, in contrast to the palladium case.[4]

Electron correlation seems to be very important in this dissociative adsorption process. Figure 5 shows the potential curve calculated by the HF method for the interaction between Pt(^1S) and H_2. Although a large stabilization is obtained relative to the Pt(^1S) + H_2 state, the stabilization energy relative to the ground state, Pt(^3D) + H_2 is only

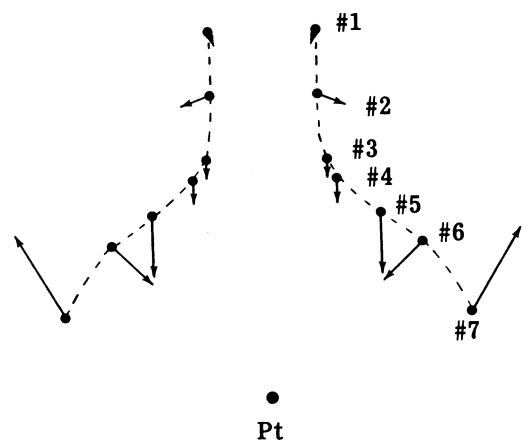

FIG. 2. Forces acting on the H atoms in the Pt–H_2 system along the reaction path shown in Fig. 1.

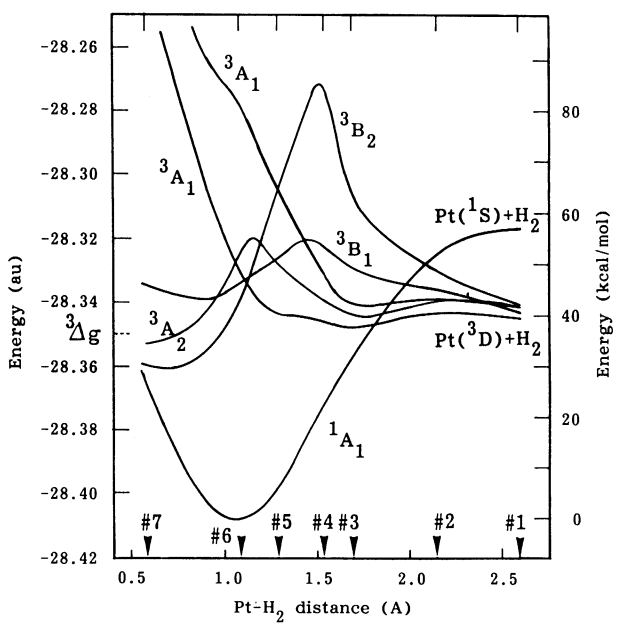

FIG. 3. Potential energy curves of the ground and excited states of the Pt–H_2 system in the side-on, on-top approach calculated by the SAC and SAC-CI methods without including spin–orbit coupling. The $^3\Delta_g$ state shown on the left-hand side is the lowest state for the linear geometry.

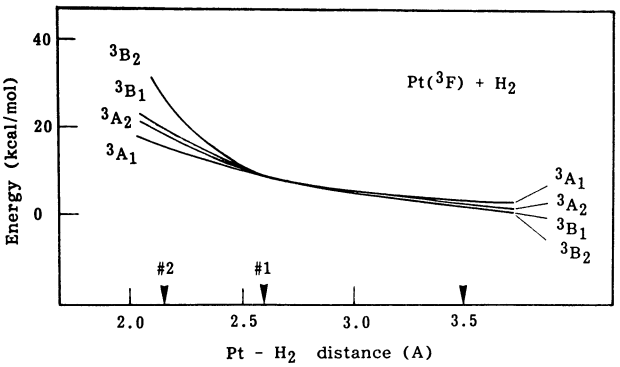

FIG. 4. Potential energy curves of the Pt–H_2 system starting from Pt(^{3}F) + H_2 calculated by the CASSCF method.

about 4 kcal/mol. This is in sharp contrast with the value, 40 kcal/mol calculated by the SAC and SAC-CI method (Fig. 3), and indicates the importance of electron correlation for the description of the dissociative adsorption. We have previously published a similar observation for the dissociative adsorption of H_2 on palladium.[4]

Next we analyze the electronic mechanism of the reaction. There are two important orbital interactions between H_2 and Pt.

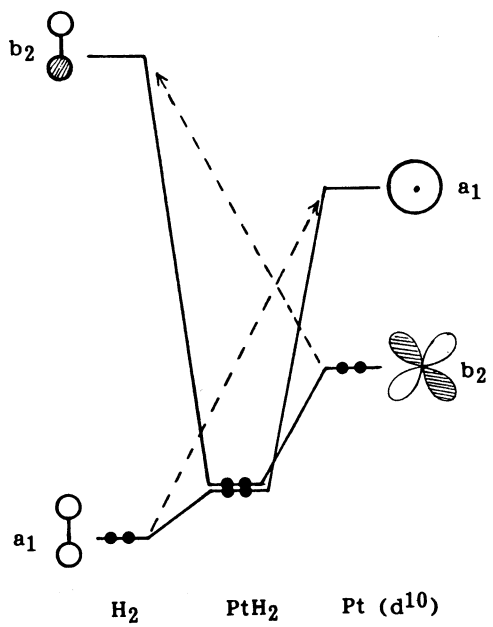

At an early stage of the interaction, electron transfer from the σ_g orbital of H_2 to the 6*s* orbital of the Pt atom is important. To accelerate the cleavage of the H–H bond, electron backtransfer from the d_{yz} orbital of the Pt atom (see Fig. 1 for the coordinate system) to the σ_u orbital of H_2 is important. The same mechanism has been found in the case of the oxidative addition of H_2 to Ni atom[1] and to $Pt(PH_3)_2$.[10] As the reaction proceeds, the electronic configuration of the Pt atom changes from d^{10} to a mixture of d^9s^1 and d^8s^2. As the Pt atom prefers the d^9s^1 and d^8s^2 configurations by 17.5 and 15.2 kcal/mol, respectively, to the d^{10} configuration,[28] this reaction proceeds very smoothly to dissociate completely the H_2 molecule. By contrast, as the Pd atom prefers the d^{10} configuration by 17.5 kcal/mol to the d^9s^1 configuration,[28] the dissociative adsorption by a single Pd atom does not occur, though it occurs smoothly on the Pd_2 cluster.[4]

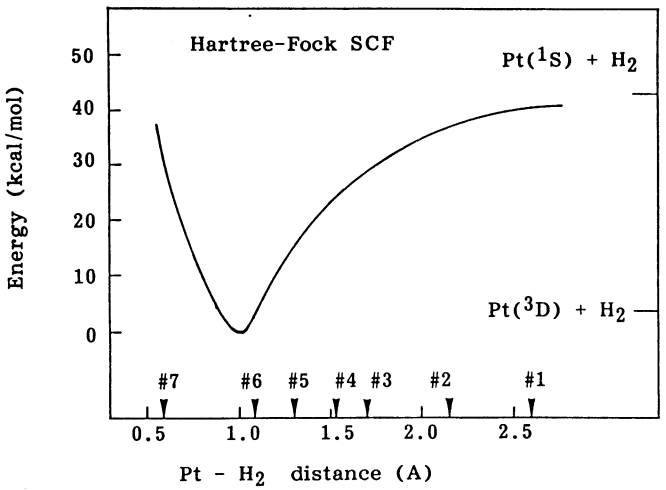

FIG. 5. Potential energy curve calculated by the Hartree–Fock method for the Pt–H_2 system starting from Pt(^1S) + H_2.

Figure 6 shows the contour maps of the density difference defined by

$$\Delta\rho = \rho(\text{Pt–H}_2) - \rho(\text{Pt}) - \rho(\text{H}) - \rho(\text{H}). \quad (4)$$

The reorganization of the electron density during the reaction course is the origin of the driving forces shown in Fig. 2.[31] Early in the reaction (1 and 2 defined in Fig. 1), the density near the hydrogens is similar to that of a free molecule. At 2, the density in the H_2 region is slightly polarized toward Pt, which induces an attractive force, acting on H, toward Pt. At 3, the Pt–H bonds are beginning to form and at 6 a typical Pt–H bond is observed with the H–H bond being completely broken.

B. Effect of spin–orbit coupling

Figure 7 shows the potential energy curves of the Pt–H_2 system calculated with including the spin–orbit coupling

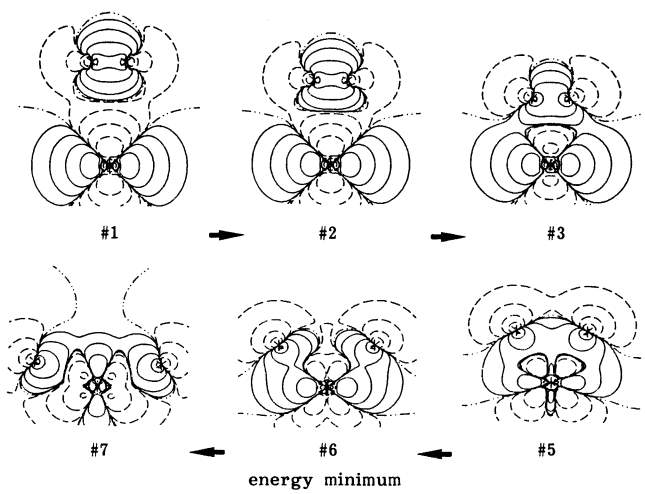

FIG. 6. Reorganization of the electron density of the Pt–H_2 system along the reaction path shown in Fig. 1. The difference density is defined by Eq. (4) of the text.

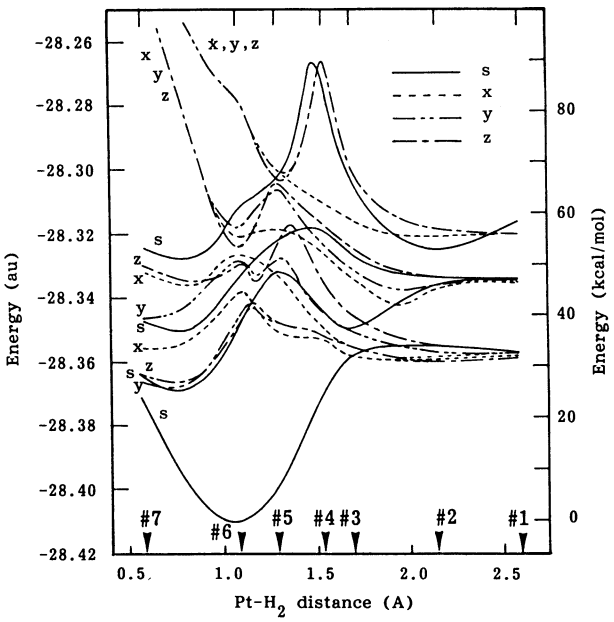

FIG. 7. Potential energy curves of the ground and excited states of the $Pt–H_2$ system in the side-on, on-top approach calculated with including spin–orbit coupling based on the SAC and SAC-CI results shown in Fig. 3.

based on the SAC/SAC-CI results shown in Fig. 3. We consider the mixing of the states arising from the interaction of H_2 with the $^1S(d^{10})$ and $^3D(d^9s^1)$ states of the Pt atom. By the inclusion of the spin–orbit coupling, the following state mixing occurs:

$$^1A_1, ^3A_2, ^3B_1, ^3B_2 \rightarrow s,$$
$$^3A_1, ^3B_1, ^2B_2 \rightarrow x,$$
$$^3A_1, ^3A_2, ^3B_1 \rightarrow y,$$
$$^3A_1, ^3A_2, ^3B_2 \rightarrow z.$$

s, x, y, and z denote the states in the jj coupling and indicate that their spin functions transform as totally symmetric and like the rotations around the axes, respectively.

Comparing Figs. 7 and 3, we see that the effect of the spin–orbit coupling is larger for the triplet states than for the singlet state. When the $Pt–H_2$ distance is large, e.g., at 1 of Fig. 7, the splitting of the triplet states is mostly due to the spin–orbit coupling in the Pt atom rather than the symmetry splitting for the system. At the intermediate and short $Pt–H_2$ distances, the symmetry splitting seems to be larger than the spin-orbit splitting. In the energy region of -28.32–-28.36 a.u., many states run rather complicatedly. For the $^1A_1$ state, the effect of the spin–orbit coupling is small when it is well separated from the other states (e.g., at 6, the effect is the lowering of about 0.002 a.u.), but when its curve comes across the A_2, B_1, and B_2 curves, a strong avoided crossing occurs due to the spin–orbit coupling. As a result, the ground state near the 6 geometry, which is essentially the $^1A_1$ state, dissociates into the lowest s state which is essentially the mixture of the $^3A_2$ and $^3B_2$ states arising from the ^3D state of the Pt atom. The heat of adsorption calculated from Fig. 7 is 32.0 kcal/mol, in comparison with the value, 40 kcal/mol, obtained without including the spin–orbit coupling. The experimental value for an extended surface is 26 kcal/mol.[30] The spin–orbit coupling effect on this value is mainly due to the large splitting of the ^3D state of the Pt atom in the infinite separation of Pt and H_2. The barrier of adsorption estimated from the ground state s curve of Fig. 7 is as small as 2.5 kcal/mol.

We thus conclude that the inclusion of the spin–orbit coupling in the $Pt–H_2$ system does not affect the main conclusion drawn from the calculations without including it: the most important state for the dissociative adsorption is the $^1A_1$ state (the lowest s state). The triplet states seem to be of little importance since the stabilization energy is about 6 kcal/mol (at near the 7 geometry), much smaller than the one for the s state, and the barrier is about 10 kcal/mol. The inclusion of the spin–orbit coupling, however, makes the behavior of the ground state curve natural when the $Pt–H_2$ distance is large.

For the $Pt_2–H_2$ and $Pt_3–H_2$ systems, we did not investigate the effect of the spin–orbit coupling. However, since all the states studied here for these systems belong to the singlet A_1 symmetry, we expect that the effect should be small as in the $Pt–H_2$ system. We can say nothing, of course, for the other states of larger spin multiplicity.

C. End-on, on-top approach

We also investigate the possibility of an end-on, on-top approach in hydrogen chemisorption on platinum. Since it is unlikely that the hydrogen molecule would be dissociated in this approach, we fix the H–H distance as equal to that of a free molecule and calculate the energy at several $Pt–H_2$ distances by the SAC and SAC-CI methods without including the spin–orbit coupling. As shown in Fig. 8, all the triplet states which arise from the interaction between the ^3D state of Pt and H_2 are repulsive towards the approach. Although the excited singlet S state is slightly attractive, no stabilization relative to the dissociation limit $Pt(^3D) + H_2$ is obtained. Thus it is concluded that the end-on approach is not favorable for the chemisorption of a hydrogen molecule on a platinum surface.

IV. $Pt_2–H_2$ SYSTEM

A. Pt_2 cluster

First, we calculate the lower-lying states of Pt_2 by the full-CI method within the 10(lower) + 2(upper) active orbital space which includes all 5d and 6s orbitals. The Pt–Pt distance is 2.746 Å which is the nearest neighbor distance in

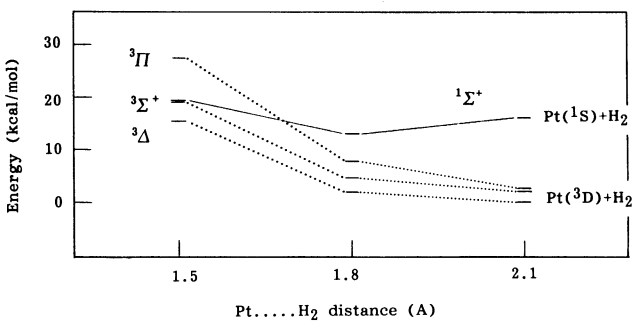

FIG. 8. Potential energy curves of the ground and excited states of the $Pt–H_2$ system in the end-on, on-top approach calculated by the SAC and SAC-CI methods.

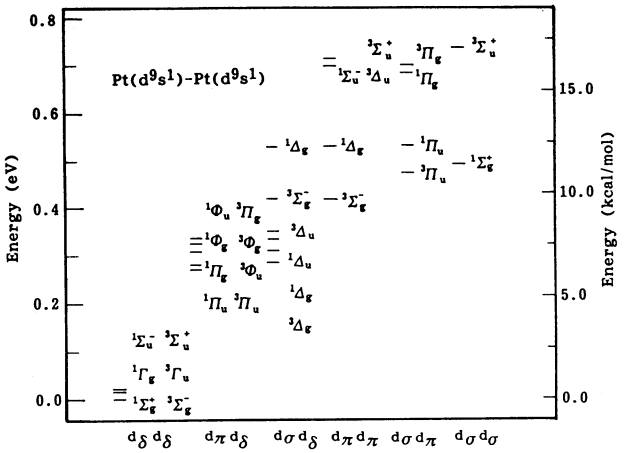

FIG. 9. Lower-lying states of Pt_2 ($R = 2.746$ Å) calculated by the full-CI method within all the 5*d* plus 6*s* active orbital space.

bulk fcc crystal.[33] The orbitals are optimized for the $^1\Gamma_g$ state by the CASSCF method with the 6 + 2 active space which does not involve the d_π orbitals. The results of the calculation are shown in Fig. 9. There are 31 states within 0.8 eV. In all of the states considered here, the Pt atoms of Pt_2 have an electronic configuration close to the median of d^9s^1 and d^8s^2, so that these states are classified into six groups by the location of the *d* holes as described for Ni_2 by Melius *et al.*[32] The $d_\delta d_\delta$ group is most stable and the six states involved in it lie within an energy range of only 0.03 eV. This is very similar to the case for Ni_2. For these six states, we perform the CASSCF calculations within the 10(lower) + 2(upper) active orbital space. As can be seen in Table II, the ground state of Pt_2 is $^3\Sigma_g^-$, but in the studyof the Pt_2–H_2 system discussed below, we consider the interaction of an H_2 molecule with the $^1\Gamma_g$ state of Pt_2, which is only 0.55 kcal/mol above the $^3\Sigma_g^-$ state.

The bonding of the Pt_2 cluster in the $^1\Gamma_g$ state is investigated by the CASSCF method with the 6 + 2 active orbital space as above. Figure 10 shows the potential energy curve of the Pt_2 cluster. The binding energy is about 27 kcal/mol, relative to the two Pt(^3D) ground state atoms. The bonding is 6*s*–6*s* and 5*d*–5*d*, but the 6*p* orbitals are not involved. The electronic configuration of the Pt atom of Pt_2 is $s^{1.5}p^{0.0}d^{8.5}$. The equilibrium bond distance is calculated at about 2.62 Å, which is slightly shorter than the distance in the bulk fcc crystal, 2.746 Å[33] to which the Pt–Pt distances in the systems Pt_2–H_2 and Pt_3–H_2 are fixed.

TABLE II. The ground state of Pt_2 ($R = 2.746$ Å) calculated by the CASSCF method.

State	E (a.u.)	ΔE (eV)	ΔE (kcal/mol)
$^3\Sigma_g^-$	− 54.226 791	0.0	0.0
$^3\Gamma_u$	− 54.226 579	0.0058	0.133
$^3\Sigma_u^+$	− 54.226 367	0.0115	0.266
$^1\Sigma_g^+$	− 54.226 107	0.0186	0.430
$^1\Gamma_g$	− 54.225 916	0.0238	0.550
$^1\Sigma_u^-$	− 54.225 680	0.0302	0.698

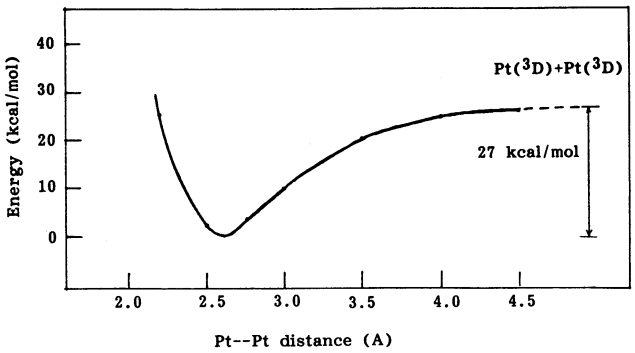

FIG. 10. Potential energy curve of the $^1\Gamma_g$ state of Pt_2 calculated by the CASSCF method.

B. Side-on, on-top approach

In Sec. IV A, we found that a hydrogen molecule is dissociated by a single Pt atom. Here we consider the adsorption process of a hydrogen molecule on the Pt_2 cluster. New aspects here are the migration process of a hydrogen atom on a Pt surface and the stability of the Pt–Pt bond during the catalytic process. The electronic structure of the Pt_2–H_2 system studied here is $^1A_1$ which arises from the interaction of Pt_2 ($^1\Gamma_g$) with H_2. The reaction path is shown in Fig. 1. The metal atoms considered here are Pt_a and Pt_b, with the Pt–Pt distance being fixed at 2.746 Å. The symmetry of the system is C_s. The points 1–6 are the same as those described for the Pt–H_2 system. After reaching position 6, which is very close to the optimized geometry of the Pt–H_2 system, we consider surface migration of the dissociated H atom. The H atom on the left-hand side is fixed at this geometry and only the H atom on the right-hand side is moved from 6 to 12. This is the migration process of a hydrogen atom from Pt_a to Pt_b. The points 9–12 lie on a circle, with Pt_b as its center and a radius of 1.53 Å; 8 is midway between points 6 and 9. The forces acting on the H atoms, calculated by the CASSCF method, are shown in Fig. 11. When the second Pt_b atom is introduced, the right H atom at 6 is pulled by Pt_b and repelled by Pt_a. The forces acting on the right H at points 8 to 10 are almost all directed along the reaction path, suggesting that hydrogen migration on the Pt_2 "surface" is favorable. At 11 and 12 this hydrogen is pulled towards Pt_b. On the other hand, the forces acting on the left H are small on moving from 6 to 12, in comparison with those acting on the right H, validating the assumption made in fixing the left H at this position.

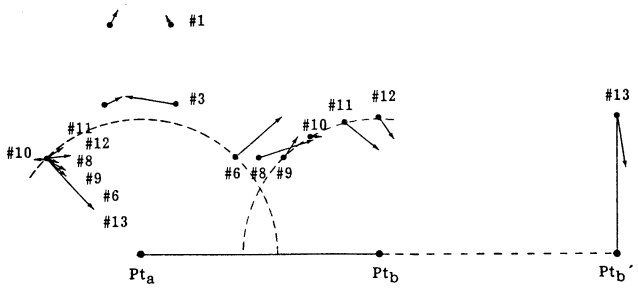

FIG. 11. Forces acting on the H atoms in the Pt_2–H_2 system along the reaction path shown in Fig. 1.

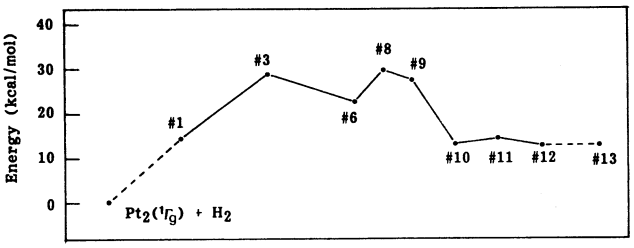

FIG. 12. Potential energy diagram of the singlet ground state of the Pt_2–H_2 system calculated by the CASSCF method.

Figure 12 shows the corresponding energetics for the adsorption and the migration processes of H_2 on Pt_2. The H_2 molecule must overcome the high barrier of 27.7 kcal/mol on going from the free system to point 3. The repulsive forces calculated at 1 and 3 in Fig. 3 correspond to this barrier. Even after reaching point 6, which is almost identical to the most stable geometry for the Pt–H_2 system, the system does not stabilize relative to the free system. This is very different from the Pt–H_2 system. Further, as the right H migrates on the Pt_2 surface from point 6 to 10, the energy of the system is lowered by about 15 kcal/mol, with the barrier of about 8 kcal/mol. Points 10–12 have almost the same energy. The adsorption energy calculated for this system is -12 kcal/mol which is the energy difference between 10 and the free system, $Pt_2(^1\Gamma_g) + H_2$. Thus all of the processes considered for this system prove to be a game at an energy level higher than the free $Pt_2 + H_2$ system. This implies that the dissociative adsorption reaction of H_2 does not occur on the Pt_2 cluster, at least in the side-on, on-top form and also in the side-on bridge form as shown below.

Another important aspect of the model study of chemisorption on a cluster surface is the stability of the cluster during catalytic processes. In order to examine this point, we calculate the energy of point 13 in Fig. 1, where the Pt_a–Pt_b distance is 5.492 Å, twice the original length of 2.746 Å, with the right H atom just above Pt_b. If any bonding remains between Pt_a and Pt_b after the migration of the H atom (at 12), the energy of 13 would become higher than that of 12. However, the calculated results shown in Fig. 12 indicate that the energy of 13 is almost the same as that of 12, implying that the Pt_a–Pt_b bond is completely broken after the hydrogen migration.

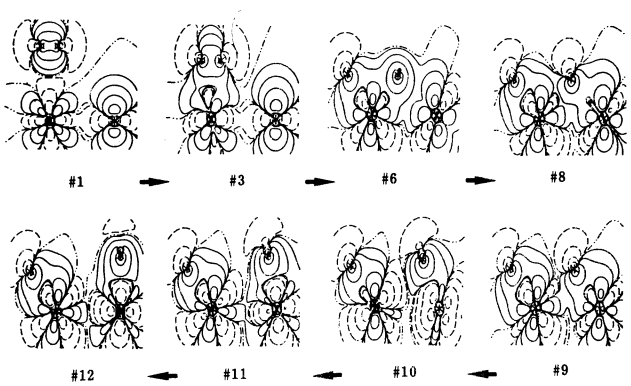

FIG. 13. Reorganization of the electron density of the Pt_2–H_2 system along the reaction path shown in Fig. 1. The difference density is defined by Eq. (5) of the text.

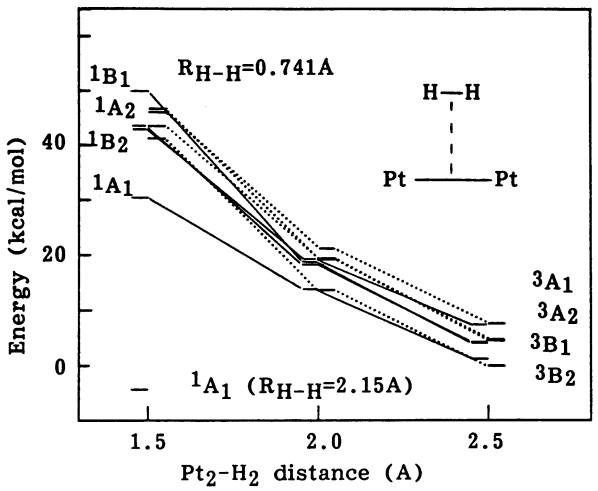

FIG. 14. Potential energy diagram of the singlet and triplet states of the Pt_2–H_2 system in the side-on, bridge-site approach calculated by the CASSCF method.

We thus conclude that the Pt_2 cluster does not react with the H_2 molecule and hence it is not a good model for chemisorption of a hydrogen molecule.

Figure 13 shows contour maps of the difference density defined by

$$\Delta\rho = \rho(Pt_2\text{–}H_2) - \rho(Pt_2) - \rho(H) - \rho(H). \quad (5)$$

For Pt_2, we use the density for the $^1\Gamma_g$ state. Even early in the adsorption (1 and 3), the electron density is diminished in the bonding region of the two Pt atoms, i.e., the cleavage of the Pt–Pt bond begins even at an early stage of the hydrogen molecule adsorption. The density in the Pt–Pt region is shifted into the Pt–H bond region and in the lone pair region of the adjacent Pt atom. The formation extent of the Pt–H bond is, on the other hand, less in the Pt_2–H_2 system than in the Pt–H_2 system as seen from Figs. 6 and 13. Thus, the high energy barrier in the initial stage of the reaction shown in Fig. 12 is due to the cleavage of the Pt–Pt bond occurring then. If we had assumed a reaction path which relaxes the Pt–Pt distance, the energy barrier early in the reaction might have been lowered.

C. Side-on, bridge-site approach

Here we examine the side-on, bridge-site approach of H_2 to Pt_2 as illustrated in Fig. 14. We first calculate the potential energy of the system by the CASSCF method as a function of the Pt_2–H_2 distance, the H–H distance of the H_2 molecule being fixed to that of a free molecule. The active space consists of 7 + 2 orbitals composed from the 5*d*, 6*s*, and 1*s*(H) AOs except for the two lowest a_1 (H and d_π) MOs, two d_δ (b_1 and a_2) MOs having nodes on H, and highest antibonding $\sigma(b_2)$ MO. As shown in Fig. 14, all the lower-lying singlet and triplet states of Pt_2 are repulsive towards the H_2 approach. Although the energy of the $^1A_1$ state is lowered to nearly the same level as that of the free system $Pt_2 + H_2$, when the H–H distance is elongated to 2.15 Å with the Pt_2–H_2 distance of 1.5 Å, more detailed calculations shown in Fig. 15 confirm that no reaction paths having a small energy barrier exist to reach there.

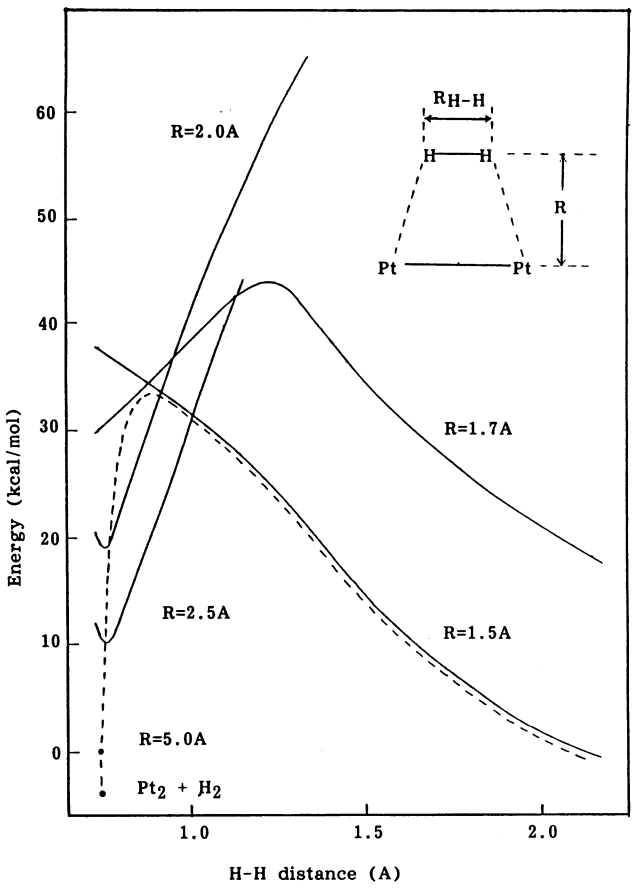

FIG. 15. Potential energy curves of the $^1A_1$ state of the Pt_2–H_2 system in the side-on, bridge-site approach calculated by the CASSCF method as a function of the H–H distance of the H_2 molecule at several distances from the Pt_2 fragment.

Figure 15 depicts the potential energy curves of the $^1A_1$ state, the lowest singlet state in Fig. 14, plotted as a function of the H–H distance for the Pt_2–H_2 distance fixed at 2.5, 2.0, 1.7, and 1.5 Å. At 5.0 Å and infinite separation, the energy is shown only for the H–H distance of the free H_2 molecule. When the H_2 molecule approaches Pt_2, it experiences a strong energy barrier. When a lower envelope of the potential curves is taken, the curve shown by the broken line in the figure is obtained, which may correspond to the most probable path for the bridge-site, side-on approach of H_2 to Pt_2. In this approach the energy barrier of chemisorption is more than 30 kcal/mol. Thus we conclude that chemisorption of an H_2 molecule on a Pt surface does not occur by the side-on, bridge-site approach. This result is similar to the case for a Ni surface studied by Siegbahn *et. al.*,[1,2] but in contrast to the case for a Pd surface studied by Nakatsuji *et. al.*[4]

V. Pt_3–H_2 SYSTEM

A. Pt_3 cluster

Last, we study the reaction of the Pt_3 cluster with the H_2 molecule, starting with an investigation of the electronic structure of the Pt_3 cluster. The geometry of the Pt_3 cluster studied here is linear as shown in Fig. 1 with the Pt–Pt distance fixed at 2.746 Å. The lower-lying states of the Pt_3 cluster are calculated by the full-CI method within the 15(lower) + 2(upper) active orbital space. The lower 15 orbitals involve all the occupied MOs and the upper two orbitals are the lowest σ MOs. The orbitals used are those optimized for the $^1\Gamma_g$ state by the CASSCF method. The active space there is the 7(lower) + 2(upper) MO space in which all the π MOs and the two bonding d_δ MOs are eliminated from the full CI space. The electronic structures of the Pt_3 cluster may be classified into two groups. One involves a hole in the occupied π orbitals and the other has fully occupied π orbitals. The ground state in the former group is shown to be unstable by about 12 kcal/mol relative to the one in the latter. So, we make CASSCF calculations within the 7(lower) + 2(upper) active orbital space for the latter group. After the interaction with H_2, the system has C_{2v} symmetry, so the energies of the lowest singlet states belonging to the four irreducible representations of C_{2v} are calculated. The results are listed in Table III. The three lowest singlet states have the same energies within the accuracy of the present calculation. The corresponding triplet states also have very similar energies. Below, we consider the interaction of H_2 with the $^1\Sigma_g$ state. The binding energy of the Pt_3 cluster, relative to the three Pt atoms in the ^3D ground state, is about 20 kcal/mol for all the states studied here, so that we may assign about 10 kcal/mol to each Pt–Pt bond. Thus, although the linear Pt_3 cluster does exist stably, its Pt–Pt bond should be weaker than that of the Pt_2 cluster. The bonding in the Pt_3 cluster is 6*s*–6*s* and 5*d*–5*d*, but the bonding σ–p_σ–σ (σ is *s* plus d_σ of the terminal Pt) is also important. The atomic configuration is $s^{0.7}p^{0.5}d^{8.5}$ for the central atom and $s^{1.6}p^{0.06}d^{8.5}$ for the terminal atoms.

TABLE III. The ground state of Pt_3 calculated by the CASSCF method.

State $D_\infty h$ (C_{2v})	E (a.u.)	ΔE[a] (kcal/mol)
$^1\Sigma_g^+$ ($^1A_1$)	− 81.304 65	− 19.9
$^1\Sigma_u^-$ ($^1A_2$)	− 81.304 85	− 19.9
$^1\Gamma_g$ ($^1B_1$)	− 81.304 65	− 19.9
$^1\Gamma_u$ ($^1B_2$)	− 81.300 72	− 17.5
$^3\Gamma_u$ ($^3A_2$)	− 81.304 63	− 19.9
$^3\Sigma_u^+$ ($^3B_2$)	− 81.304 62	− 19.9
$^3\Sigma_g^-$ ($^3B_1$)	− 81.304 62	− 19.9
$^3\Delta_g$ ($^3A_1$)	− 81.301 53	− 18.0

[a] $\Delta E = E(Pt_3) - 3E[Pt(^3D)]$.

B. Side-on, on-top approach

Here we examine, using a larger cluster Pt_3, the dissociative adsorption of an H_2 molecule and the migration of an H atom on a platinum surface. The reaction path is again the side-on, on-top approach shown in Fig. 1 and all of the three Pt atoms Pt_a, Pt_b, and Pt_c are involved. The geometries of the approach 1–12 are the same as those defined and used previously for the Pt–H_2 and Pt_2–H_2 systems. The ground state of the Pt_3 cluster, the $^1\Sigma_g^+$ state, is allowed to react with the H_2 molecule. The potential energy curve for the singlet A_1 state is calculated by the MC-SCF method within the 5(lower) + 3(upper) active orbital space generating all of

the SDTQ (single, double, triple, and quadruple) excited configurations. The active space involves four d_δ orbitals and four σ orbitals relevant to the reaction process. The MC-SCF calculation has been performed with the lower 61 MOs, leaving the upper 18 MOs frozen as the HF MOs.[25] The results are shown in Fig. 16. The energy of 1, where the Pt_3–H_2 distance is 2.6 Å, is lower than that of the free system, Pt_3 ($^1\Sigma_g$) + H_2 by 5.0 kcal/mol, probably indicating a physisorption state. At point 2, the system is unstabilized by 4.7 kcal/mol in comparison with 1, but this is almost at the same energy level as the free system. The energy barrier which has to be overcome is considerably smaller in this system than in the previous Pt_2–H_2 system. At point 6, which is close to the most stable geometry of the Pt–H_2 system, the energy lowering from the free system is 15.7 kcal/mol. Although this is smaller than that of the Pt–H_2 system (about 40 kcal/mol), it is larger than that of the Pt_2–H_2 system (− 21.9 kcal/mol). As the right H atom migrates on the Pt_3 surface from 6 to 11, the energy of the system is lowered again by 15.6 kcal/mol, with no energy barrier. The system prefers one H atom on each Pt atom rather than two H atoms on one Pt atom. The adsorption energy finally calculated for this system is 31.3 kcal/mol. This is obtained by subtracting the energy of 11 from that of the free system Pt_3 ($^1\Sigma_g$) + H_2. This energy may be compared with the experimental adsorption energy, 24 kcal/mol of H_2 on a real Pt surface.[22]

We next examine the strength of the Pt–Pt bond during the migration process, as in the case of the Pt_2–H_2 system. At 13, the Pt_a–Pt_b distance is elongated to 5.492 Å, twice of the original distance, with the right H atom kept on the Pt_b atom. The energy at 13 is higher than that at 11 by 23.3 kcal/mol, ensuring that even after the migration a reasonably strong bond exists between Pt_a and Pt_b. In contrast to the Pt_2 case, the stability of the Pt_3 cluster is related to the existence of the nonbonding σ MO which is considerably stabilized by the participation of the p_σ AO of the central Pt atom.

We thus conclude that the Pt_3 cluster reacts with the H_2 molecule as

$$\text{Pt–Pt–Pt} + \text{H}_2 \rightarrow \text{Pt–}\overset{\text{H}\ \text{H}}{\underset{|\ \ |}{\text{Pt}}}\text{–Pt}$$

essentially without an energy barrier. This reaction gives a rather good model for the actual surface reaction both in reproducing the adsorption energy and in showing the stability of the Pt–Pt bond during the dissociative adsorption process.

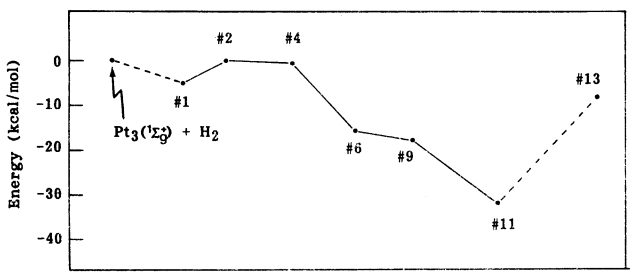

FIG. 16. Potential energy diagram of the singlet A_1 state of the Pt_3–H_2 system calculated by the MC-SCF method.

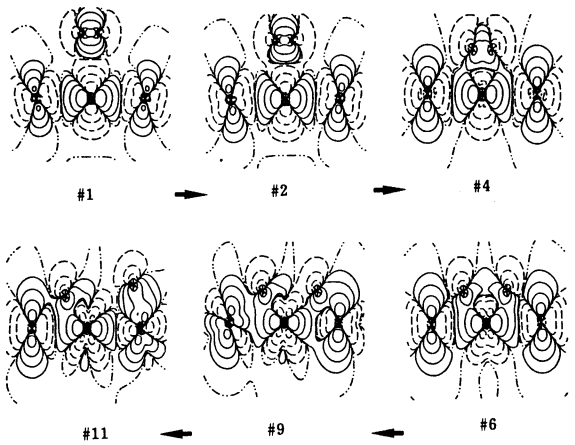

FIG. 17. Reorganization of the electron density of the Pt_3–H_2 system along the reaction path shown in Fig. 1. The difference density is defined by Eq. (6) of the text.

The changes in the electron density along the reaction path are displayed in Fig. 17. The maps are defined by the electron density difference,

$$\Delta\rho = \rho(\text{Pt}_3\text{–H}_2) - \rho(\text{Pt}_3) - \rho(\text{H}) - \rho(\text{H}). \qquad (6)$$

For the Pt_3 cluster, we use the density of the $^1\Sigma_g^+$ state. As the H_2 molecule approaches Pt_a, the density around Pt_a gradually extends toward it in a manner very similar to that found for the previous Pt–H_2 system, whereas the density around Pt_b and Pt_c shows hardly any change. At point 6, a bond is clearly formed between Pt_a and H, but some bonding still remains between the two H atoms. This differs from the Pt–H_2 case where the H–H bond is completely broken at point 6. Thus as seen from the stability of 6 relative to the free system, the activity of the central Pt atom toward dissociation of the H–H bond is lower in the Pt_3 cluster than in the Pt atom, due to the existence of the Pt–Pt bonds. It is noteworthy that even in the interaction with the Pt_3 cluster, essentially only the central Pt atom participates in the initial dissociative adsorption process. We further note that the density in the Pt–Pt region does not decrease in the Pt_3–H_2 system, though it is reorganized, in contrast to the Pt_2–H_2 system shown in Fig. 13 (compare 2 or 4 with the previous 3). As the right H atom migrates from Pt_a to Pt_b, a bond is gradually formed between this H and Pt_b. At point 9, a weak bond is also formed between Pt_c and the left H fixed at the same position as in 6. This participation of the left Pt_c in the migration process onto the right Pt_b would be a reason for the nonexistence of an energy barrier in the migration process in contrast to the Pt_2–H_2 case. At all of the points except for 9, the density around Pt_c and in the bonding regions of Pt_a–Pt_b and Pt_a–Pt_c hardly changes. The gross charge of the H atom is slightly positive throughout the process, for example, + 0.09 at 6 and + 0.05 (average) at 11.

The forces acting on the hydrogen along the reaction path from point 1 to 11 are shown in Fig. 18. These forces reflect the behavior of the density shown in Fig. 17.[31] At 4, where the H–H distance is optimized for the Pt–H_2 system, the force is directed toward Pt_a. If Pt_b and Pt_c were to cooperate with Pt_a in the initial dissociative adsorption step of H_2, the force at this point might have been directed toward

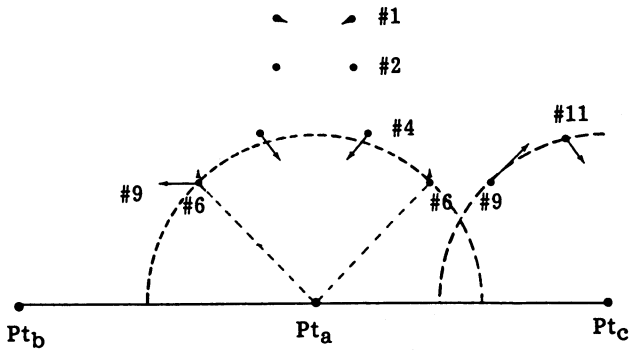

FIG. 18. Forces acting on the H atoms in the Pt_3–H_2 system during the dissociative and the migration steps from 1 to 11 shown in Fig. 1.

these atoms. The force at 9 acts parallel to the migration path toward the terminal Pt atom. That is, after the H_2 molecule is dissociatively adsorbed by a single Pt atom, the neighboring Pt atoms begin to pull the H atoms toward them.

VI. SUMMARY AND CONCLUDING REMARKS

In this paper, an *ab initio* theoretical study of the reactions of a hydrogen molecule with small platinum clusters, Pt_n ($n = 1,2,3$) has been reported. For the Pt_3 cluster, a linear geometry was assumed. We predicted that the Pt atom and the Pt_3 cluster would react smoothly with H_2, but the Pt_2 cluster would not. In the former case, the H–H bond was broken and the Pt–H bond was formed. In particular, the reaction with the Pt_3 cluster appeared suitable as a model of hydrogen chemisorption on an actual platinum surface. The calculated heat of reaction was 40 kcal/mol (32 kcal/mol with including the spin–orbit coupling) for the Pt–H_2 system, -12 kcal/mol for the Pt_2–H_2 system, and 32 kcal/mol for the Pt_3–H_2 system, in comparison with the experimental value, 26 kcal/mol for an extended surface.[30] We examined some possible approaches of a hydrogen molecule to the Pt clusters and found that the side-on, on-top approach to a surface Pt atom is the most probable path. The migration of H after dissociative adsorption occurred very smoothly, without an energy barrier. The Pt–Pt bond of the Pt_3 cluster was stable during these processes. Experiments must now be undertaken on the reactivity of the small Pt clusters.

We first found that a single Pt atom did "catalyze" cleavage of the H–H bond. The catalytically active state was not the ground $^3D(d^9S^1)$ state, but the excited $^1S(d^{10})$ state of the Pt atom. When the spin–orbit coupling was included, we obtained the natural potential curve connecting the adsorbed system (almost singlet A_1 Pt–H_2) and the separate system (almost triplet D state of Pt and H_2). The other lower-lying states of the Pt atom were repulsive toward the H_2 molecule. The mechanism of the catalytic cleavage was essentially the same as that of the well-known oxidative addition of a hydrogen molecule to a Pt complex.[10] The $5d$ orbital of the Pt atom was seen as very important for dissociating the H–H bond and for forming the two Pt–H bonds, through an electron transfer from the d_{yz} orbital to the antibonding σ_u MO of H_2. The role of electron correlation was also significant. The effect of the spin–orbit coupling was, however, relatively insignificant, because the lowest, catalytically most active state was the singlet A_1 state.

We next studied the reaction of H_2 and Pt_2, examining not only the adsorption process, but also the migration process of an H atom on the Pt_2 surface. A large energy barrier of about 23 kcal/mol was calculated for the initial dissociative adsorption step, and a stabilization of about 10 kcal/mol for the migration step of a hydrogen atom from PtH_2–Pt to PtH–PtH. Therefore, no net stabilization was obtained, so that the Pt_2–H_2 system would not be a good model of hydrogen chemisorption on a Pt surface. Furthermore, the Pt–Pt bond was shown to be completely broken after the migration process. The effect of the spin–orbit coupling was not examined for this Pt_2–H_2 and the following Pt_3–H_2 system. We expect that the effect would be small at least for the singlet state studied in this paper.

The linear cluster Pt_3 was found to react smoothly with H_2. A shallow minimum of about 5 kcal/mol was found in the very initial stage and seemed to correspond to a physisorption state. The hydrogen molecule was then dissociatively adsorbed in the side-on, on-top approach on a single Pt atom of the Pt_3 cluster. The stabilization due to this process was about 16 kcal/mol. No energy barrier existed for the migration of an H atom from the two coordination site to the adjacent one coordination site. The energy lowering in this process was about 16 kcal/mol. The net stabilization was therefore about 32 kcal/mol. The Pt–Pt bond was stable during the chemisorption process. These facts all verified that the Pt_3 cluster was a good model for the hydrogen chemisorption on a real surface.

Within the nickel triad, Ni, Pd, and Pt, the reactivity of Pt towards hydrogen chemisorption is similar to that of Ni, rather than that of Pd.[1–5] The catalytic activity of Pt seems to be higher than that of Ni. For Ni and Pt, the dissociative adsorption of an H_2 molecule occurs in the side-on, on-top approach without passing through a molecular adsorption state. In contrast, Pd adsorbs H_2 in the side-on, bridge-site approach, both in molecular and dissociative forms, with the latter being more stable than the former by a few kcal/mol.[4]

After submission of this manuscript, the paper due to Balasubramanian[34] has appeared, who also pointed out that the ground state of the PtH_2 system is a bent $^1A_1$ state with the minimum geometry very similar to ours.

[1] M. R. A. Blomberg and P. E. M. Siegbahn, J. Chem. Phys. **78**, 5682 (1983).
[2] P. E. M. Siegbahn, M. R. A. Blomberg, and C. W. Bauschlicher, J. Chem. Phys. **81**, 2103 (1984).
[3] H. Nakatsuji and M. Hada, Croat. Chem. Acta, **57**, 1371 (1984).
[4] (a) H. Nakatsuji and M. Hada, J. Am. Chem. Soc. **107**, 8264 (1985); (b) H. Nakatsuji, M. Hada, and T. Yonezawa, J. Am. Chem. Soc. **109**, 1902 (1987).
[5] U. B. Brandemark, M. R. A. Blomberg, L. G. M. Petterson, and P. E. M. Siegbahn, J. Phys. Chem. **88**, 4617 (1984).
[6] (a) H. Nakatsuji and M. Hada, in *Quantum Chemistry: The Challenge of Transition Metals and Coordination Chemistry*, edited by A. Veillard (Reidel, Dordrecht, 1986), p. 477; (b) H. Nakatsuji, M. Hada, and T. Yonezawa, Surf. Sci. **185**, 319 (1987).
[7] S. W. Wang and K. S. Pitzer, J. Chem. Phys. **79**, 3851 (1983).

[8]A. Gavezzotti, G. F. Tantardini, and M. Simonetta, Chem. Phys. **84**, 453 (1984).
[9]E. Poulain, J. Garcia-Prieto, M. E. Ruiz, and O. Novaro, Int. J. Quantum Chem. **29**, 1181 (1986).
[10]J. J. Low and W. A. Goddard, J. Am. Chem. Soc. **106**, 6928 (1984); S. Obara, K. Kitaura, and K. Morokuma, *ibid.* **106**, 7482 (1984).
[11]E. Miyoshi, Y. Sakai, and S. Mori, Chem. Phys. Lett. **113**, 457 (1985).
[12]S. Tsuchiya, Y. Amenomiya, and R. J. Cvetanovic, J. Catal. **19**, 245 (1970).
[13]S. Tsuchiya and M. Nakamura, J. Catal. **50**, 1 (1977).
[14]K. Christmann, G. Ertl, and T. Pignet, Surf. Sci. **54**, 365 (1976).
[15]S. L. Bernasek and G. A. Somorjai, J. Chem. Phys. **62**, 3149 (1975).
[16]M. Salmeron, R. J. Gale, and G. A. Somorjai, J. Chem. Phys. **67**, 5324 (1977).
[17]J. O. Noell and P. J. Hay, Inorg. Chem. **21**, 14 (1982).
[18](a) S. Huzinaga, J. Chem. Phys. **42**, 1293 (1965); (b) T. H. Dunning, Jr., *ibid.* **53**, 2823 (1970).
[19](a) H. Nakatsuji, K. Kanda, and T. Yonezawa, Chem. Phys. Lett. **75**, 340 (1980); (b) H. Nakatsuji, T. Hayakawa, and M. Hada, *ibid.* **80**, 94 (1981).
[20]H. Nakatsuji and K. Hirao, J. Chem. Phys. **68**, 2053 (1978).
[21]H. Nakatsuji, Chem. Phys. Lett. **59**, 362 (1978); **67**, 329, 334 (1979).
[22]H. Nakatsuji, Chem. Phys. **75**, 425 (1983).
[23]H. Nakatsuji, No. 146 (Y4/SAC), Data Processing Center of Kyoto University, 1985; Program Library SAC85 (No. 1396), Computer Center of the Institute for Molecular Science, Okazaki, 1986.
[24]B. O. Roos, P. R. Taylor, and P. E. M. Siegbahn, Chem. Phys. **48**, 157 (1980); P. Siegbahn, A. Heiberg, B. Roos, and B. Levy, Phys. Scr. **21**, 323 (1980).
[25]M. Hada, H. Yokono, and H. Nakatsuji, Chem. Phys. Lett. **141**, 339 (1987).
[26]B. R. Brooks, P. Saxe, W. D. Laidig, and M. Dupuis, Program Library No. 481, Computer Center of the Institute for Molecular Science, 1981.
[27](a) C. A. Masmanidis, H. H. Jaffe, and R. L. Ellis, J. Phys. Chem. **79**, 2052 (1975); (b) S. Kato, R. L. Jaffe, A. Komornicki, and K. Morokuma, J. Chem. Phys. **78**, 4567 (1983).
[28]C. E. Moore, *Atomic Energy Levels* (National Bureau of Standards, Washington, D.C., 1971), Vol. 3.
[29]K. P. Huber and G. Herzberg, *Molecular Spectra and Molecular Structure. IV. Constants of Diatomic Molecules* (Van Nostrand Reinhold, New York, 1979).
[30]J. R. Anderson, *Structure of Metallic Catalysts* (Academic, New York, 1975).
[31](a) H. Nakatsuji, J. Am. Chem. Soc. **95**, 345 (1973); **96**, 24, 30 (1974); (b) H. Nakatsuji and T. Koga, in *The Force Concept in Chemistry*, edited by B. M. Deb (Van Nostrand Reinhold, New York, 1981), Chap. 3.
[32]C. F. Melius, J. W. Moskowitz, A. P. Mortola, M. B. Baillie, and M. A. Ratner, Surf. Sci. **59**, 279 (1976).
[33]*Handbook of Chemistry and Physics* (Chemical Rubber, Cleveland, 1984–1985), p. F-167.
[34]K. Balasubramanian, J. Chem. Phys. **87**, 2800 (1987).